JACS
JOURNAL OF THE AMERICAN CHEMICAL SOCIETY

Article

pubs.acs.org/JACS

Computational Design of Effective, Bioinspired HOCl Antioxidants: The Role of Intramolecular Cl^+ and H^+ Shifts

Amir Karton,[†,‡,*] Robert J. O'Reilly,[†,‡,§] David I. Pattison,[‡,∥,⊥] Michael J. Davies,[‡,∥,⊥] and Leo Radom[†,‡,*]

[†]School of Chemistry, University of Sydney, Sydney, NSW 2006, Australia
[‡]ARC Centre of Excellence for Free Radical Chemistry and Biotechnology
[∥]Heart Research Institute, 7 Eliza Street, Newtown, NSW 2042, Australia
[⊥]Faculty of Medicine, University of Sydney, Sydney, NSW 2006, Australia

Supporting Information

ABSTRACT: The enzyme myeloperoxidase generates significant amounts of hypochlorous acid (HOCl) at sites of inflammation to inflict oxidative damage upon invading pathogens. However, excessive production of this potent oxidant is associated with numerous inflammatory diseases. Recent kinetic measurements suggest that the endogenous antioxidant carnosine is an effective HOCl scavenger. On the basis of computational modeling, we suggest a possible mechanism for this antioxidant activity. We find that a unique structural relationship between three adjacent functional groups (imidazole, carboxylic acid, and terminal amine) enables an intramolecular chlorine transfer to occur. In particular, two sequential proton shifts are coupled with a Cl^+ shift converting the kinetically favored product (chlorinated at the imidazole nitrogen) into the thermodynamically favored product (chlorinated at the terminal amine) effectively trapping the chlorine. We proceed to design systems that share similar structural features to those of carnosine but with even greater HOCl-scavenging capabilities.

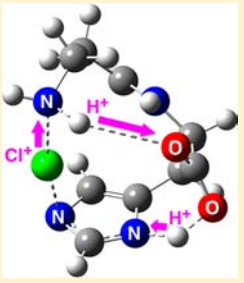

1. INTRODUCTION

Carnosine (*β*-alanyl-L-histidine) is a naturally occurring dipeptide that is synthesized from the amino acids *β*-alanine and L-histidine by the enzyme carnosine synthase. It is present in high concentrations in skeletal and heart muscle tissues, as well as in the brain and the eye lens. Numerous experimental studies on the biochemical and physiological properties of carnosine have shown that it exhibits a diverse range of health and antiageing benefits.[1,2] Carnosine is a highly effective protective agent against damage induced by a broad spectrum of toxic species, including reactive oxygen species (e.g., ·OH,[3] HOCl,[4,5] and ONOOH),[6] glycating agents,[2] and cytotoxic carbonyls (e.g., acetaldehyde,[7] formaldehyde,[7] methylglyoxal,[8] and malondialdehyde[4]). Carnosine also assumes a range of biologically important roles, including those of an intracellular pH regulator, immunostimulator, neurotransmitter, epithelializing agent, and a chelator of copper and zinc ions.[1,5] Consequently, carnosine has been shown to play a preventative role in a broad range of chronic diseases, such as cardiac disorders, cancer, diabetes, Alzheimer's disease, Parkinson's disease, osteoporosis, autism, and cataracts.[1,5]

In recent years, there has been an accumulation of evidence suggesting that carnosine may play a role in inhibiting biological damage mediated by hypochlorous acid (HOCl) by effectively removing the chlorinating equivalents.[1,4,9] At sites of inflammation, activated phagocytes (primarily neutrophils and monocytes) release the heme enzyme *myeloperoxidase*, which catalyzes the oxidation of Cl^- by H_2O_2, affording the potent oxidant HOCl.[10] Hypochlorous acid plays a key role in the innate host defense against invading pathogens by inflicting massive oxidative damage. However, excessive production of this powerful oxidant (and/or production at the wrong place or time) can damage host biological targets (such as DNA and proteins) and this has been implicated in numerous inflammatory diseases including atherosclerosis, arthritis, and some cancers.[10] Therefore, it is important to identify the mechanisms by which endogenous species can effectively scavenge HOCl and as a result rationally design exogenous agents with higher efficacy.[11] Such compounds should react with HOCl faster than HOCl reacts with primary biological targets, and the R−Cl bond that is formed should be sufficiently strong to remain intact under physiological conditions. Despite the thousands of experimental investigations regarding carnosine that have been published in the past two decades, we are not aware of any previous theoretical studies concerning the *N*-chlorinated derivatives of this intriguing dipeptide.

Carnosine has two imidazole nitrogens (N_1 and N_2, Scheme 1), an amino nitrogen (N_3), and an amido nitrogen (N_4). The N_2 imidazole nitrogen is readily chlorinated by HOCl. Kinetic measurements suggest that, subsequent to the initial chlorination at the N_2 imidazole nitrogen, a rapid intramolecular Cl transfer occurs, in which the Cl migrates to the terminal primary amine (N_3).[9,12] This suggests that the efficacy of carnosine as a protective agent may be associated with an interplay between kinetically and thermodynamically driven

Received: September 19, 2012
Published: November 13, 2012

dx.doi.org/10.1021/ja309273n | J. Am. Chem. Soc. 2012, 134, 19240−19245

Scheme 1. Chlorination of Carnosine at the Imidazole Nitrogen and Subsequent Intramolecular Cl Transfer to the Terminal Primary Amino Nitrogen

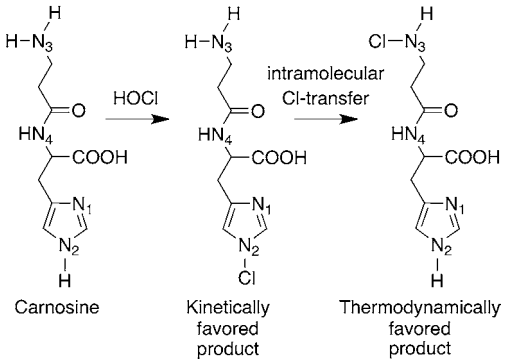

processes. That is, initial chlorination occurs at the imidazole nitrogen (the kinetically favored site), followed by an intramolecular Cl transfer in which the Cl is transferred to the terminal primary amino nitrogen (the thermodynamically favored site). Of relevance to this issue is a recent systematic evaluation of N−Cl bond dissociation energies in molecules containing a wide range of biologically important functional groups using high-level ab initio calculations.[13] It was found that the strength of an N−Cl bond (with respect to homolysis) increases in the order: imidazole < free amine < amide.[13a] For example, the MeHN−Cl bond is predicted to be stronger than the imidazole−N−Cl bond by 42.7 kJ mol^{-1} (at 0 K). On this basis, the Cl transfer from the imidazole to the amino moiety in *N*-chlorinated carnosine is expected to be appreciably exothermic.

In the present work, we examine the mechanism for the intramolecular Cl shift from the imidazole ring to the terminal amine in *N*-chlorinated carnosine using the high-level G4(MP2) thermochemical procedure.[14] We show that the interplay between three simple functional groups (NH_2, COOH, and imidazole) can lead to a relatively low-lying transition structure (TS) for the chlorine migration. In particular, two proton shifts are coupled with an intramolecular Cl^+ shift. The present work goes on to examine systems that share similar structural features with carnosine and shows that the proposed mechanism is not limited to carnosine. Indeed, the barrier for the Cl^+ migration can be significantly reduced by increasing the length of the β-alanyl-glycyl side-chain.

2. COMPUTATIONAL METHODS

High-level ab initio[15] and density functional theory[16] calculations were carried out using the *Gaussian 09* and *Gaussian 03* program suites.[17] Geometries and vibrational frequencies were obtained in a simulated aqueous environment at the B3-LYP/6-31G(2df,p) level of theory. Bulk solvent effects in the geometry and frequency calculations were included using the charge-density-based SMD continuum solvation model,[18] with this level of theory denoted SMD-(water)-B3-LYP/6-31G(2df,p). Zero-point vibrational energy, enthalpic, and entropic corrections have been obtained from such calculations. The equilibrium structures were verified to have all real harmonic frequencies and the transition structures to have only one imaginary frequency. The connectivities of the transition structures were confirmed by performing intrinsic reaction coordinate (IRC) calculations.[19] Gas-phase Gibbs free energies at 298 K were obtained using the G4(MP2) variant of the Gaussian-4 (G4) composite thermochemical protocol,[14] using the SMD(water)-B3-LYP/6-31G(2df,p) optimized geometries. Relative energies in the text refer to the combination of an SMD(water)-M05-2X/6-31G(d) solvation correction on top of the G4(MP2)//SMD(water)-B3-LYP/6-31G(2df,p) energy (where the SMD single-point calculations were carried out at the M05-2X/6-31G(d) level of theory, as recommended by Marenich, Cramer and Truhlar[18]). For the sake of brevity, this level of theory is denoted SMD(water)-G4(MP2).

G4(MP2) has been found to produce gas-phase thermochemical properties (such as reaction energies, bond dissociation energies, and enthalpies of formation) with a mean absolute deviation (MAD) of 4.4 kJ mol^{-1} from the experimental energies of the G3/05 test set.[20] It has been recently found that G4(MP2) shows a similarly good performance for barrier heights.[21,22]

To check on the sensitivity of the solvation corrections to the choice of the model, we have also carried out calculations using the conductor-like polarizable continuum model (CPCM).[23] The CPCM single-point calculations were carried out at the HF/6-31+G(d) level of theory in conjunction with UAHF atomic radii, as recommended by Takano and Houk.[24] The SMD and CPCM solvation models predict similar solvation energies and lead to the same qualitative trends. Thus, solvation energies obtained from the two models agree on average to within 3.8 kJ mol^{-1}. The main text reports the SMD results, while the CPCM results for carnosine are presented in Table S1 of the Supporting Information.

3. RESULTS AND DISCUSSION

3.1. Role of Intramolecular Cl^+/H^+ Shifts in the HOCl Antioxidant Activity of Carnosine. High-level ab initio calculations (with the G4(MP2) thermochemical protocol) were performed in a simulated aqueous environment in order to explore the potential energy surface (PES) for the intramolecular Cl transfer in carnosine (Computational Methods section). The multistep reaction path for the chlorine migration proceeds by way of three consecutive intramolecular steps, which are schematically illustrated in Figure 1. The three

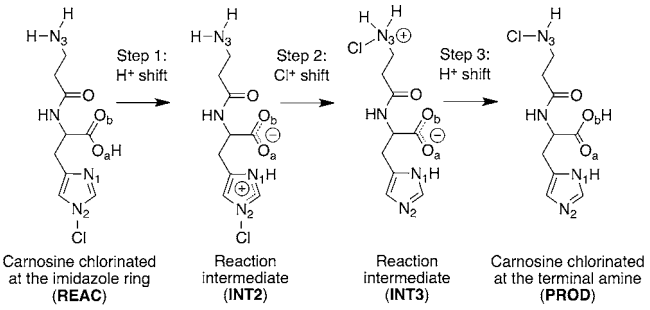

Figure 1. Schematic representation of the intramolecular rearrangements involved in the Cl^+ transfer from the imidazole nitrogen (N_2) to the terminal amino nitrogen (N_3).

steps are: (i) a proton shift from the carboxylic acid oxygen (O_a) to the adjacent imidazole nitrogen (N_1), (ii) a Cl^+ shift from the imidazole nitrogen (N_2) to the nitrogen of the terminal amine (N_3), and (iii) a proton shift from the terminal amino nitrogen (N_3) to the carboxylate oxygen (O_b). The first proton shift results in a zwitterionic intermediate (**INT2**) in which the carboxylate group is negatively charged and the imidazole ring is positively charged. The subsequent Cl^+ shift

dx.doi.org/10.1021/ja309273n | J. Am. Chem. Soc. 2012, 134, 19240−19245

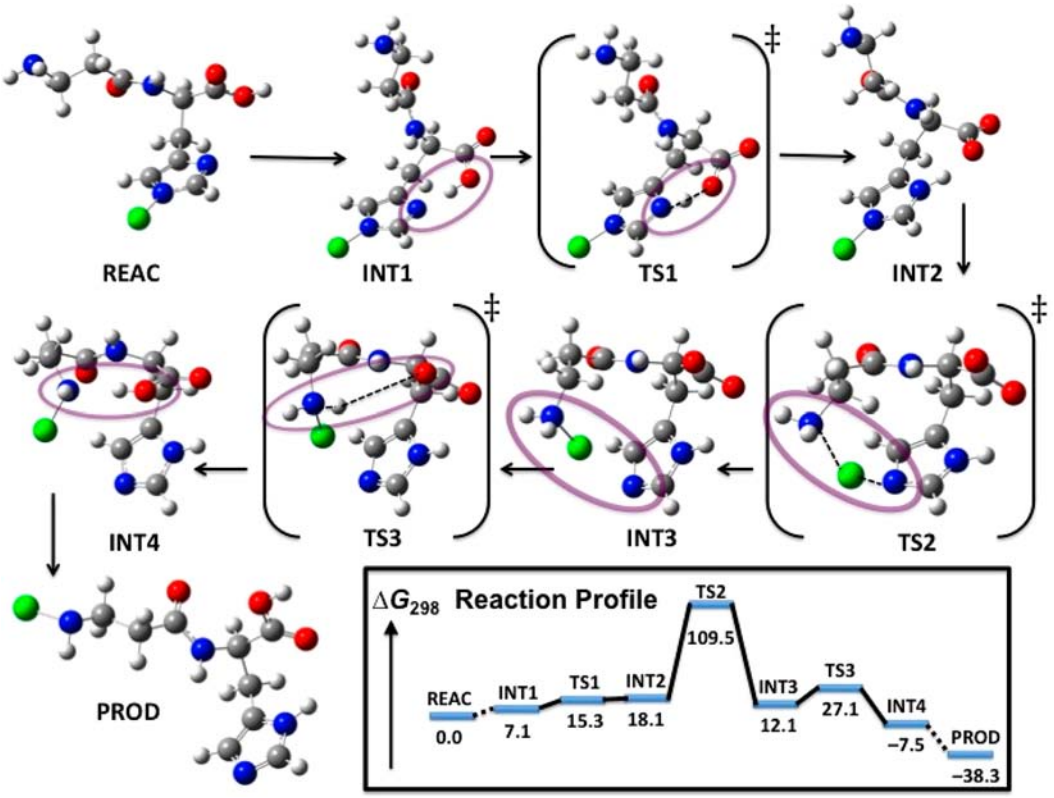

Figure 2. Schematic Gibbs free-energy reaction profile for the intramolecular Cl^+ transfer in *N*-chlorinated carnosine (ΔG_{298}, SMD(water)-G4(MP2), kJ mol^{-1}). Atomic color scheme: H, white; C, gray; N, blue; O, red; Cl, green. The bonds being broken and formed in the transition structures are represented by black dashed lines.

results in a second zwitterion intermediate (**INT3**) in which the positive charge is located on the terminal amino group (Figure 1). It should be noted that in aqueous solution under physiological conditions the reactant (**REAC**) would be expected to exist predominantly in its zwitterionic form (RNH_3^+, $R'COO^-$), which does not allow for a unimolecular chlorine shift to proceed.[25] However, the proposed mechanism can proceed through the portion of the population in the nonzwitterionic form, as shown in Figure 1.

The equilibrium and transition structures that were located on the reaction path are shown in Figure 2 along with the schematic representation of the Gibbs free-energy surface (ΔG_{298}, SMD(water)-G4(MP2), kJ mol^{-1}). The lowest energy conformation of carnosine chlorinated at N_2 of the imidazole ring is labeled as the reactant (**REAC**) and was chosen as the zero-energy reference point of the reaction profile. In this conformation, the β-alanyl-glycyl side chain is directed away from the histidine residue, and the formamide moiety of the peptide backbone (C(=O)NH) and the carboxylic acid (C(=O)OH) are almost coplanar (e.g., the ∠O=C···C=O dihedral angle between the two carbonyl groups is 167.6°). The first reaction intermediate (**INT1**) lies higher in energy than the minimum-energy conformation by 7.1 kJ mol^{-1}. The structurally important conformational change that occurs between **REAC** and **INT1** is that the carboxylic acid moiety adopts the higher-energy trans configuration, allowing the OH group to form a hydrogen bond with the adjacent imidazole nitrogen N_1 (with an $O_aH\bullet\bullet\bullet N_1$ distance of 1.623 Å, and an $\angle O_aHN_1$ angle of 169.3°, **INT1** in Figure 2). The transition structure (**TS1**) for the first proton shift (from the carboxyl group to the imidazole ring) lies only 15.3 kJ mol^{-1} above the starting reactant (**REAC**). The ensuing zwitterionic intermediate (**INT2**) constitutes the starting point for the Cl^+ shift.[26]

The migration of Cl^+ from the imidazole ring to the terminal amine is the key for the potent HOCl-antioxidant activity of carnosine, as it results in effective trapping of the chlorine. In particular, chlorine is transferred from the kinetically preferred site (the imidazole nitrogen, N_2) to the thermodynamically preferred site (the primary terminal amino nitrogen, N_3). The transition structure (**TS2**) for this step lies 109.5 kJ mol^{-1} above the minimum-energy conformation of the reactant (**REAC**) and leads to the third reaction intermediate (**INT3**). The transition structure (**TS3**) for the second proton transfer (from the terminal amino group to the carboxylate group) lies 27.1 kJ mol^{-1} above the starting reactant (**REAC**). The resulting reaction intermediate (**INT4**) lies lower in energy than the reactant (**REAC**) by 7.5 kJ mol^{-1}. However, the minimum-energy conformation of the product (**PROD**) lies 38.3 kJ mol^{-1} below the reactant (Figure 2). This means that, in any secondary intermolecular Cl transfer in which *N*-chlorinated carnosine may participate with nitrogen-containing functional groups of other biologically important targets, the reaction of carnosine chlorinated at the terminal nitrogen (**PROD**) would be more endergonic (or less exergonic) by 38.3 kJ mol^{-1} than the reaction with carnosine chlorinated at the imidazole nitrogen (**REAC**).

The relative Gibbs free energy of the TS for the Cl^+ shift (ΔG_{298}(**TS2**) = 109.5 kJ mol^{-1}) lies significantly higher than that for the first proton shift (ΔG_{298}(**TS1**) = 15.3 kJ mol^{-1}) and the second proton shift (ΔG_{298}(**TS3**) = 27.1 kJ mol^{-1}). Because the Cl^+ transfer is clearly the rate-determining step (RDS) for the overall process, we will focus in the next sections

dx.doi.org/10.1021/ja309273n | *J. Am. Chem. Soc.* 2012, 134, 19240−19245

primarily on this step. The transition structure **TS2** enables the imidazole nitrogen (N_2) and the primary amino nitrogen (N_3) to be in relatively close proximity (with an $N_2\cdots N_3$ distance of 4.2 Å). In particular, the Cl atom is sandwiched between the two nitrogens such that the $N_2\cdots Cl$ distance is 1.797 Å and the $Cl\cdots N_3$ distance is 2.558 Å. In this structure, the Cl atom accommodates a partial positive charge, the atomic polar tensor (APT) charge[27] on the Cl atom being +0.96. On the other hand, the carboxylate group accommodates a partial negative charge (e.g., the APT charge on the $COO^{\delta-}$ group is −0.92). Because of this increased degree of charge separation in the transition structure (the dipole moment of **TS2** being 13.9 D) relative to the reactant (the dipole moment of **REAC** being 4.9 D), the reaction barrier is expected to increase as the polarity of the solvent decreases. For example, the Gibbs free-energy barrier for the Cl^+ shift in the gas phase ($\Delta G^{\ddagger}_{298,gas}$) is 186.1 kJ mol^{-1}.

The results above indicate that the likely involvement of explicit water molecules in the proton shifts is not expected to significantly affect the dynamics of the *overall* reaction as the transition structures for the proton-transfer steps (**TS1** and **TS3**) lie significantly lower in energy than the transition structure for the chlorine shift (**TS2**). This suggests that the reaction would occur also in a polar aprotic solvent such as acetonitrile. In fact, such experiments would provide a valuable test of our proposed water-independent mechanism. The experimental investigations reported to date have been carried out only in aqueous solution under physiological conditions.[4,9]

3.2. Antioxidants with Improved HOCl Scavenging Capabilities. The results described above set the stage for designing HOCl antioxidants that share similar structural features with carnosine but with a reduced barrier for the intramolecular chlorine transfer. In the present work, we consider structural modifications of the β-alanyl-glycyl side chain. Figure 3 shows the candidates that are considered, in

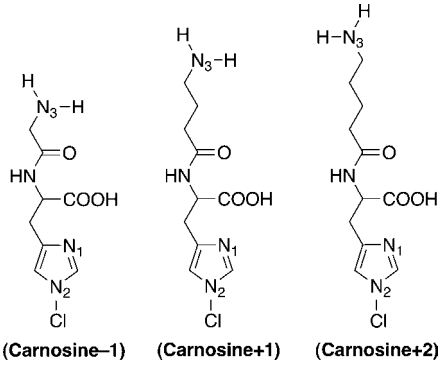

Figure 3. Candidates considered for HOCl-antioxidants with potentially reduced barriers for the intramolecular Cl^+ transfer.

which the length of the β-alanyl-glycyl side chain has been: (i) shortened by one carbon (carnosine−1), (ii) increased by one carbon (carnosine+1, homocarnosine), and (iii) increased by two carbons (carnosine+2).

Table 1 gives the overall Gibbs free-energy barriers ($\Delta G^{\ddagger}_{298}$) and reaction free energies (ΔG_{298}) for the chlorine-transfer reactions for chlorinated carnosine and the related systems shown in Figure 3, while the TSs for the chlorine transfer in these systems are displayed in Figure 4. Shortening the side chain by one carbon (carnosine−1, Figure 3) results in a substantial increase in the barrier (by 27.6 kJ mol^{-1} relative to

Table 1. Gibbs Free-Energy Barriers and Reaction Energies ($\Delta G^{\ddagger}_{298}$ and ΔG_{298}, SMD(water)-G4(MP2), kJ mol^{-1}) for the Intramolecular Cl^+ Transfer in the *N*-Chlorinated Derivatives of Carnosine and the Related Systems in Figure 3

	$\Delta G^{\ddagger}_{298}$ [a]	ΔG_{298} [a]
carnosine−1	137.1	−43.6
carnosine	109.5	−38.3
carnosine+1	66.4	−43.0
carnosine+2	49.4	−42.3

[a] $\Delta G^{\ddagger}_{298}$ and ΔG_{298} values are calculated relative to the minimum-energy conformation of the reactant; $\Delta G^{\ddagger}_{298}$ corresponds to the relative energy of the TS for the rate-determining step, i.e., the intramolecular Cl^+ shift.

carnosine). This is consistent with the experimental observation that, under physiological conditions, the intramolecular Cl shift fails to occur in the carnosine−1 dipeptide.[9] However, increasing the length of the side chain by one carbon (carnosine+1) decreases the barrier by 43.1 kJ mol^{-1} relative to that in carnosine. A further increase in the length of the chain by one more carbon (carnosine+2) results in a barrier decrease by 17.0 kJ mol^{-1} relative to that in carnosine+1. Inspection of the chlorine-transfer TSs for these systems (Figure 4) reveals that increasing the length of the β-alanyl-glycyl side-chain allows the TSs for the Cl^+ transfer to become earlier (i.e., less distorted) and therefore lower in energy. In particular, as the length of the side chain is increased, the Cl atom can remain closer to the plane of the imidazole ring. This is indicated, for example, by angles ($\angle N_1CN_2Cl$) between the plane of the imidazole ring and the N_2−Cl bond of 64.5° (carnosine−1), 50.4° (carnosine), 39.9° (carnosine+1), and 27.7° (carnosine+2) (Figure 4). In addition, the N_2−Cl bond distances decrease in the same order, specifically they are: 1.853 (carnosine−1), 1.797 (carnosine), 1.790 (carnosine+1), and 1.743 (carnosine+2) Å (compared with an N_2−Cl distance of 1.700 Å in **REAC**).[28]

Further inspection of Figure 4 shows that increasing the length of the β-alanyl-glycyl side-chain in carnosine by one or two carbons also provides the conformational flexibility for a more effective hydrogen bond to be formed between the negatively charged $COO^{\delta-}$ and positively charged $H{-}N_1^{\delta+}$ moieties. This is demonstrated by $COO^{\delta-}\cdots HN_1^{\delta+}$ distances of 2.258 (carnosine), 1.678 (carnosine+1), and 1.673 (carnosine+2) Å, and by the bond angles around the hydrogen bond (Table S2 of the Supporting Information). Thus, the trends in the Gibbs free-energy barriers, namely carnosine ≫ carnosine+1 ∼ carnosine+2, may in part be associated with the formation of a more effective intramolecular hydrogen bond between the charged carboxylate and $H{-}N_1$ moieties.

4. CONCLUSIONS

On the basis of our computational modeling, we have been able to propose a mechanism for the intramolecular Cl shift in carnosine that emerges from a unique structural relationship between three adjacent functional groups, namely, the imidazole ring, carboxylic acid, and primary amine moieties. The interplay between these functional groups enables two concerted intramolecular proton shifts to be coupled with an intramolecular Cl^+ shift (as shown in Figure 2). The Cl^+ shift is found to be the rate-determining step, with a barrier of 109.5 kJ mol^{-1} relative to the reactant, in which carnosine is chlorinated

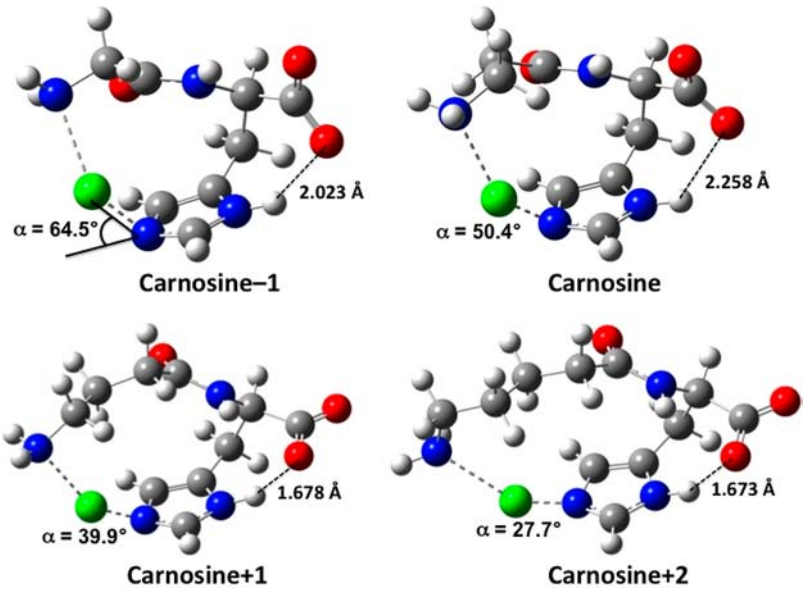

Figure 4. Transition structures obtained at the SMD(water)-B3-LYP/6-31G(2df,p) level of theory for the intramolecular Cl^+ transfer in *N*-chlorinated carnosine and the related systems shown in Figure 3. Atomic color scheme: H, white; C, gray; N, blue; O, red; Cl, green. The ∠ N_1CN_2Cl angle (α) between the plane of the imidazole ring and the N_2−Cl bond is given in degrees and the length of the H-bond distance $COO^{\delta-}\cdots HN_1^{\delta+}$ is given in Å (text).

in the imidazole ring. As the transition structures for the proton shifts lie significantly lower in energy than the transition structure for the Cl^+ shift, the likely involvement of explicit water molecules in the proton shifts is not expected to significantly affect the dynamics of the overall reaction. Therefore, the chlorine migration is expected to proceed also in a polar aprotic solvent. Finally, we find that the proposed reaction mechanism also applies to structurally related systems in which the length of the β-alanyl-glycyl side-chain is varied. In particular, increasing the length of the β-alanyl-glycyl side-chain leads to a substantial reduction in the barrier height for the Cl^+ shift and therefore to antioxidants with potentially greater HOCl-scavenging capabilities.

■ ASSOCIATED CONTENT

Supporting Information

Gas-phase reaction profile for the intramolecular Cl^+ transfer in *N*-chlorinated carnosine; CPCM results for the reaction profile for the intramolecular Cl^+ transfer in *N*-chlorinated carnosine; bond distances and angles around the $COO^{\delta-}\cdots HN_1^{\delta+}$ H-bonds for the species shown in Figure 4; SMD(water)-B3-LYP/6-31G(2df,p) optimized geometries for the species considered in the present work; G4(MP2)//SMD(water)-B3-LYP/6-31G(2df,p) total energies and M05-2X/6-31G(d) SMD solvation energies in aqueous solution for the species considered in the present work; and full references for the *Gaussian 09* and *Gaussian 03* program suites. This material is available free of charge via the Internet at http://pubs.acs.org.

■ AUTHOR INFORMATION

Corresponding Author

*radom@chem.usyd.edu.au; amir.karton@chem.usyd.edu.au

Present Address

[§]School of Chemistry, University of Tasmania, Private Bag 75, Hobart TAS 7001, Australia.

Notes

The authors declare no competing financial interest.

■ ACKNOWLEDGMENTS

We gratefully acknowledge funding (to AK and LR) from the Australian Research Council, and the generous allocation of computing time from the National Computational Infrastructure (NCI) National Facility and from Intersect Australia Ltd.

■ REFERENCES

(1) Hipkiss, A. R. *Adv. Food Nutr. Res.* **2009**, *57*, 87−154.
(2) Reddy, V. P.; Garrett, M. R.; Perry, G.; Smith, M. A. *Sci. Aging Knowl. Environ.* **2005**, *2005*, 12.
(3) Tamba, M.; Torreggiani, A. *Int. J. Radiat. Biol.* **1999**, *75*, 1177−1188.
(4) Hipkiss, A. R.; Worthington, V. C.; Himsworth, D. T. J.; Herwig, W. *Biochim. Biophys. Acta* **1998**, *1380*, 46−54.
(5) Quinn, P. J.; Boldyrev, A. A.; Formazuyk, V. E. *Mol. Aspects Med.* **1992**, *13*, 379−444.
(6) Fontana, M.; Pinnen, F.; Lucente, G.; Pecci, L. *Cell. Mol. Life Sci.* **2002**, *59*, 546−555.
(7) Hipkiss, A. R.; Preston, J. E.; Himsworth, D. T. M.; Worthington, V. C.; Keown, M.; Michaelis, J.; Lawrence, J.; Mateen, A.; Allende, L.; Eagles, P. A. M.; Abbott, N. J. *Ann. N.Y. Acad. Sci.* **1998**, *854*, 37−53.
(8) Hipkiss, A. R.; Chana, H. *Biochem. Biophys. Res. Commun.* **1998**, *248*, 28−32.
(9) Pattison, D. I.; Davies, M. J. *Biochemistry* **2006**, *45*, 8152−8162.
(10) (a) Klebanoff, S. J. *J. Leukocyte Biol.* **2005**, *77*, 598−625. (b) van der Veen, B. S.; de Winther, M. P. J.; Heeringa, P. *Antioxid. Redox Signal.* **2009**, *11*, 2899−2937. (c) Davies, M. J.; Hawkins, C. L.; Pattison, D. I.; Rees, M. D. *Antioxid. Redox Signal.* **2008**, *10*, 1199−1234. (d) Nicholls, S. J.; Hazen, S. L. *Arterioscler. Thromb. Vasc. Biol.* **2005**, *25*, 1102−1111. (e) Ohshima, H.; Tatemichi, M.; Sawa, T. *Arch. Biochem. Biophys.* **2003**, *417*, 3−11.
(11) (a) Hussain, H. H.; Babic, G.; Durst, T.; Wright, J. S.; Flueraru, M.; Chichirau, A.; Chepelev, L. L. *J. Org. Chem.* **2003**, *68*, 7023−7032. (b) Zhang, H.-Y.; Sun, Y.-M.; Wang, X.-L. *Chem.—Eur. J.* **2003**, *9*, 502−509. (c) Zhang, H.-Y.; Yang, D.-P.; Tang, G.-Y. *Drug Discovery Today* **2006**, *11*, 749−754. (d) Liu, Z.-Q. *Chem. Rev.* **2010**, *110*, 5675−5691. (e) Winterbourn, C. C. *Nat. Chem. Biol.* **2008**, *4*, 278−286.

(12) Pattison, D. I.; Davies, M. J. *Chem. Res. Toxicol.* **2001**, *14*, 1453−1464.
(13) (a) O'Reilly, R. J.; Karton, A.; Radom, L. *J. Phys. Chem. A.* **2011**, *115*, 5496−5504. (b) O'Reilly, R. J.; Karton, A.; Radom, L. *Int. J. Quantum Chem.* **2012**, *116*, 1862−1878.
(14) Curtiss, L. A.; Redfern, P. C.; Raghavachari, K. *J. Chem. Phys.* **2007**, *127*, 124105-1−124105-8.
(15) Hehre, W. J.; Radom, L.; Schleyer, P. v. R.; Pople, J. A. *Ab Initio Molecular Orbital Theory*; Wiley: New York, 1986.
(16) Koch, W.; Holthausen, M. C. *A Chemist's Guide to Density Functional Theory*, 2nd ed.; Wiley: New York, 2001.
(17) (a) Frisch, M. J. et al..; *Gaussian 03, revision E.01*; Gaussian, Inc.: Wallingford CT, 2003. (b) Frisch, M. J. et al..; *Gaussian 09, revision B.01*; Gaussian, Inc.: Wallingford CT, 2009.
(18) Marenich, A. V.; Cramer, C. J.; Truhlar, D. G. *J. Phys. Chem. B* **2009**, *113*, 6378−6396.
(19) (a) Gonzalez, C.; Schlegel, H. B. *J. Chem. Phys.* **1989**, *90*, 2154−2161. (b) Gonzalez, C.; Schlegel, H. B. *J. Phys. Chem.* **1990**, *94*, 5523−5527.
(20) Curtiss, L. A.; Redfern, P. C.; Raghavachari, K. *J. Chem. Phys.* **2005**, *123*, 124107-1−124107-12.
(21) (a) Zheng, J.; Zhao, Y.; Truhlar, D. G. *J. Chem. Theory Comput.* **2009**, *5*, 808−821. (b) Karton, A.; Tarnopolsky, A.; Lamere, J.−F.; Schatz, G. C.; Martin, J. M. L. *J. Phys. Chem. A* **2008**, *112*, 12868−12886.
(22) Curtiss, L. A.; Redfern, P. C.; Raghavachari, K. *Chem. Phys. Lett.* **2010**, *499*, 168−172.
(23) Cossi, M.; Rega, N.; Scalmani, G.; Barone, V. *J. Comput. Chem.* **2003**, *24*, 669−681.
(24) Takano, Y.; Houk, K. N. *J. Chem. Theory Comput.* **2005**, *1*, 70−77.
(25) Based on density functional theory calculations (SMD(water)-M06−2X/6-311+G(3df,2p)), the transition structure for the proton transfer from the R′COOH group to the RNH_2 group lies 14.9 kJ mol^{-1} above **REAC** and the zwitterionic form of **REAC** lies 23.6 kJ mol^{-1} below **REAC**.
(26) Note that on the SMD(water)-G4(MP2) Gibbs free-energy surface, the intermediate (**INT2**) lies 2.8 kJ mol^{-1} above the transition structure (**TS1**). However, on the SMD(water)-B3-LYP/6-31G(2df,p) Gibbs free-energy surface, **INT2** lies 1.4 kJ mol^{-1} below **TS1**.
(27) (a) Cioslowski, J. *J. Am. Chem. Soc.* **1989**, *111*, 8333−8336. (b) De Proft, F.; Martin, J. M. L; Geerlings, P. *Chem. Phys. Lett.* **1996**, *250*, 393−401. (c) Note that according to a natural population analysis (NPA), the positive charge on the Cl atom is significantly smaller (i.e. +0.17) and the charge on the $COO^{\delta-}$ group is −0.82.
(28) Note that increasing the length of the β-alanyl-glycyl side chain by one more carbon (carnosine+3) follows the same trend, i.e., it results in a TS with α = 14.5° and an N_2−Cl bond length of 1.702 Å, and, based on density functional theory calculations (SMD(water)-M06−2X/6-311+G(3df,2p)), the barrier is estimated to decrease by 19.9 kJ mol^{-1} relative to the barrier in carnosine+2 (Table S2 of the Supporting Information).